Sharafaldeen and Abdelatif
Journal of Engineering and Applied Science (2024) 71:83
https://doi.org/10.1186/s44147-024-00409-7

Journal of Engineering and Applied Science

RESEARCH

Open Access

3D non-linear finite element modeling of one-way RC slab strengthened with concrete overlay

Muaaz Sharafaldeen[1] and Amged O. Abdelatif[2*]

*Correspondence:
Amged.Abdelatif@uofk.edu

[1] Building and Road Research Institute, University of Khartoum, Khartoum, Sudan
[2] Department of Civil Engineering, University of Khartoum, B.O. Box 321, Khartoum, Sudan

Abstract

Reinforced concrete (RC) slabs often require strengthening due to deterioration, increased loads, or design changes. Concrete overlay is a commonly used technique for strengthening, but predicting the behavior of overlays can be challenging. To address this challenge, this study presents a three-dimensional non-linear finite element model using Abaqus/CAE to analyze the structural performance of one-way reinforced concrete (RC) slabs strengthened with concrete overlays. The model considers three different bonding conditions at the interface: friction, epoxy, and shear connectors. The predictions of the model were compared to experimental results, and it was found that the model accurately captures the load–deflection response, cracking behavior, and interfacial slip in the strengthened slabs. Additionally, the model accurately predicts the new structural capacity of the strengthened slabs, showing good agreement with experimental data. These findings offer valuable insights into the effectiveness of concrete overlays as a traditional strengthening technique for RC slabs. Moreover, the developed finite element model provides a useful tool for optimizing the design of these overlays.

Keywords: Reinforced concrete, Slabs, Overlay, Flexural strengthening, Finite element modeling

Introduction

The field of strengthening and upgrading existing structures has seen significant growth due to advancements in construction techniques and the need for quality control. The demand for exploring this field has grown, especially after structural failures and requests for building alterations from clients [1]. Strengthening concrete elements is crucial to address issues such as damage, design errors, functional changes, and corrosion [2]. Among the various methods available for strengthening concrete slabs, such as Ferro-cement covers [3], section enlargement, external plate bonding [4], external post-tensioning [5], span shortening, supplemental members, load reduction, and fiber-reinforced polymers [6–8], this research focuses on concrete overlay [9–11].

Concrete overlay involves applying a layer of concrete onto an existing reinforced concrete (RC) slab to enhance its structural performance. This technique is commonly used but predicting the behavior of overlays can be challenging [1]. Therefore, this study aims to improve understanding of the behavior of RC slabs strengthened with concrete overlays through the use of the non-linear finite element (FE) method.

Background

Reinforced concrete (RC) overlay strengthening is a well-established technique that offers numerous benefits, including the use of cost-effective materials, excellent fire resistance, and the elimination of skilled labor [12]. Furthermore, it provides sufficient warning prior to failure [2]. The effectiveness of RC overlay strengthening relies heavily on the bond strength between the overlay and the substrate [9]. As a result, researchers have dedicated their efforts to studying various substrate surface preparation techniques that enhance the interfacial shear strength for optimal composite action between the overlay and substrate [12, 13]. These studies have examined factors such as overlay thickness [11], distribution of shear connectors [12], strength of the overlay concrete, surface roughening methods, and more [13].

Experiments generally show increased stiffness, strength, and load-carrying capacity of RC slabs with overlay strengthening [8, 9, 12]. Full composite action and monolithic behavior are achieved when there is proper surface preparation and adequate shear transfer between the overlay and substrate [9]. However, debonding and lack of composite action can occur without adequate bonding or shear connectors between the layers [12]. More connectors or surface roughening is often needed to achieve full composite action [8]. Recent studies have shown that ultra-high-performance fiber concrete (UHPFC) and high-strength concrete (HSC) overlays can strengthen reinforced concrete slabs in flexure [14, 15]. These overlays significantly increase flexural strength compared to un-strengthened slabs. However, UHPFC and HSC overlays can be costly for some applications. In a recent study, a numerical model was developed to predict the behavior of reinforced concrete slabs strengthened with concrete overlays using various bonding techniques [16]. The model takes into account the non-linear behavior of concrete by utilizing an interpolation method based on Eurocode 2 using MATLAB software. However, advancements in FE modeling could result in better visualization and tracking of stress and slip at the interface.

Overall, while experimental studies on one-way slabs strengthened by concrete overlays have been extensively conducted, numerical studies are still limited but gaining traction [16]. The development of numerical models could significantly enhance our understanding of the behavior of strengthened slabs and provide valuable insights into the effects of different design parameters and bonding techniques.

Methods

To achieve the objective of this study, a 3D non-linear FE model using Abaqus/CAE 2017 [17] was developed to simulate the behavior of an RC one-way slab strengthened with a concrete overlay considering different bonding conditions at the interface. The model can offer a reliable tool for predicting the structural performance of strengthened RC slabs, allowing for optimization of the design process. The model will be developed and validated using the geometry and material properties of previous experimental works in literature [2].

Experiments procedure

The previous experimental study tested five slabs to examine the structural efficacy of the concrete overlay strengthening technique [2]. The first slab, referred to as the Original RC Slab (OS), measures 55 cm in width, 200 cm in length, and 8 cm in thickness. It is reinforced with 10 mm rebar spaced every 160 mm in both directions (Fig. 1). The second, third, and fourth slabs, known as Strengthened Slabs (SS), were strengthened using a 50-mm concrete overlay with Ø6@160 mm c/c each way (Fig. 2). The primary difference between these three slabs lies in the bonding condition at the interface between the original slab and overlay. The bonding methods used were friction, epoxy material, and shear keys (shear connectors), respectively. The fifth slab, also a strengthened slab, differs in that the concrete overlay is reinforced using Ø8 instead of Ø6 and is connected to the original slab using shear keys. In this study, these five slabs are referred to as OS, SS-T6-Friction, SS-T6-Epoxy, SS-T6-Shear Keys, and SS-T8-Shear Keys. The characteristics of slabs are summarized in Table 1.

The slabs were prepared using steel reinforcement with a yield stress of 460 N/mm2 and concrete that was designed to achieve a compressive strength of 30 N/mm2. The concrete mix was prepared using a water-cement ratio of 0.47 and the following mix proportions: 435 kg/m3 of cement, 205 kg/m3 of water, 730 kg/m3 of fine aggregates, and 970 kg/m3 of coarse aggregates.

The slabs were subjected to testing in a simply supported setup, with the supports placed 190 cm apart, as depicted in Fig. 3. A line load was applied at the midpoint of the span until the slab reached its failure point.

Modeling geometry

In this study, five models were developed, each one corresponding to a slab that was tested. These models are OS, SS-T6-Friction, SS-T6-Epoxy, SS-T6-Shear Keys, and SS-T8-Shear Keys.

In ABAQUS [17] (Fig. 4), both the concrete and reinforcement parts of the original slab and overlay were created as independent 3D deformable solid elements. These elements were subsequently combined in the assembly module. The concrete was modeled using eight-node tetrahedral quadratic brick elements with reduced integration, of type C3D8R. The steel reinforcement was represented by 2-node truss elements of type T3D2. Both parts were subjected to a simulation with a mesh size of 15 mm.

Modeling bond between slab and overlay

In this study, full bond action between steel reinforcement and concrete is assumed. It is modeled using the embedded element feature in ABAQUS [17] which involves embedding steel reinforcement truss elements within concrete brick elements (i.e., the host) [18].

The bond conditions between the original slab and the concrete overlay are modeled in distinct ways depending on the specific circumstances. In scenarios where the bond relies solely on friction, the interaction between the reinforced concrete (RC)

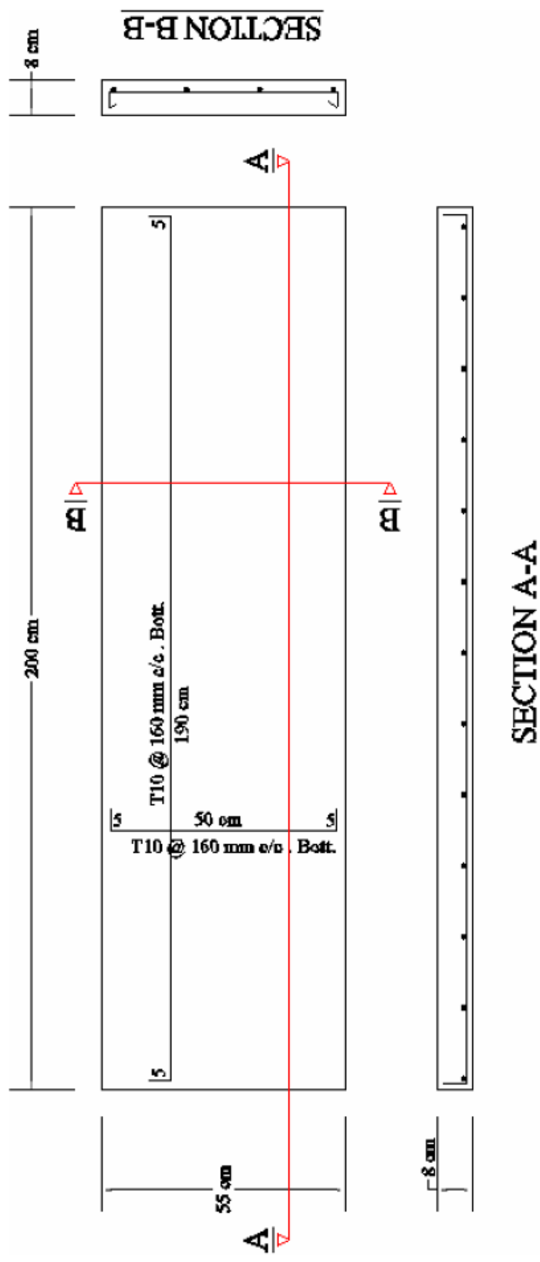

Fig. 1 Structural details of the original RC slab [2]

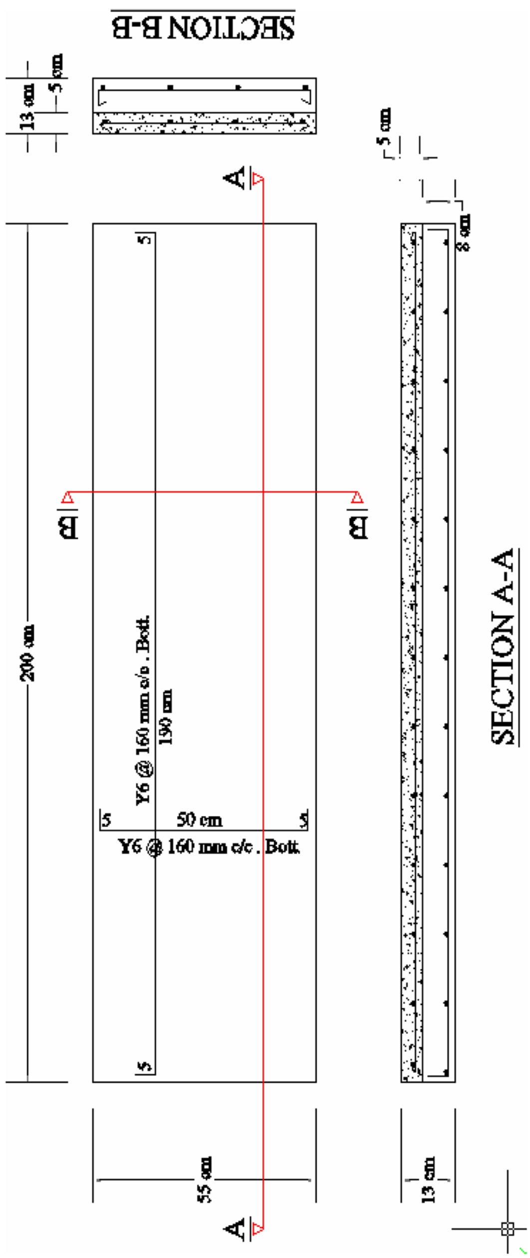

Fig. 2 Structural details of the concrete overlay used for strengthening slabs 2, 3, and 4 [2]

Table 1 Characteristics of slabs

No	Slab ID	Reference slab		Bonding condition at interface	RC overlay	
		Dimensions (cm)	Reinforcement		Dimensions (cm)	Reinforcement
1	OS	200 × 55 × 8	Ø10@160 mm both ways	–	200 × 55 × 5	Ø6@160 mm both ways
2	SS-T6-Friction			Friction		
3	SS-T6-Epoxy			Epoxy Material of 36 MPa bond strength		
4	SS-T6-Shear Keys			Shear keys (6Ø12 mm/shear span)		
5	SS-T8-Shear Keys					Ø8@160 mm both ways

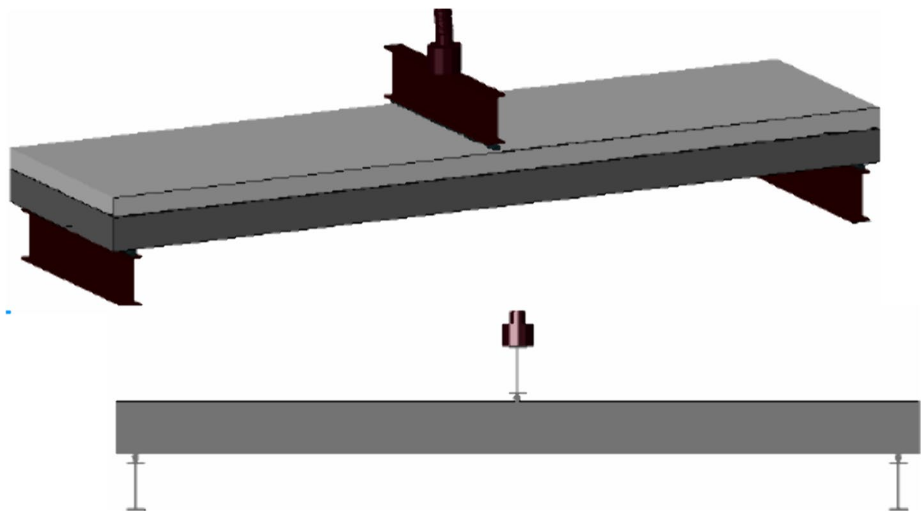

Fig. 3 One-way slab strengthened using concrete overlay under line load [2]

slab and the concrete overlay is modeled using a surface-to-surface contact element type. Here, the Coulomb friction model is utilized, assuming a friction coefficient of 0.8 [19].

When Epoxy adhesion is used, the interaction between the two surfaces is modeled as a tie constraint, where full bond action is assumed. In this case, each node on the top surface of the RC slab (i.e., the slave surface) is tied to a point on the bottom surface of the overlay (i.e., the master surface). In the case of Shear keys, the shear keys themselves are modeled as truss members embedded in both the RC slab and the overlay at the prescribed locations. The bond in the remaining part of the slab is modeled similarly to the friction case.

Slip between surfaces is expected to occur when the tangential friction exceeds a specified tolerance of 0.5% of the average length of the contact elements in the model [20]. To solve normal and tangential contact behaviors, an augmented Lagrange multiplier algorithm and penalty method in ABAQUS are employed [17].

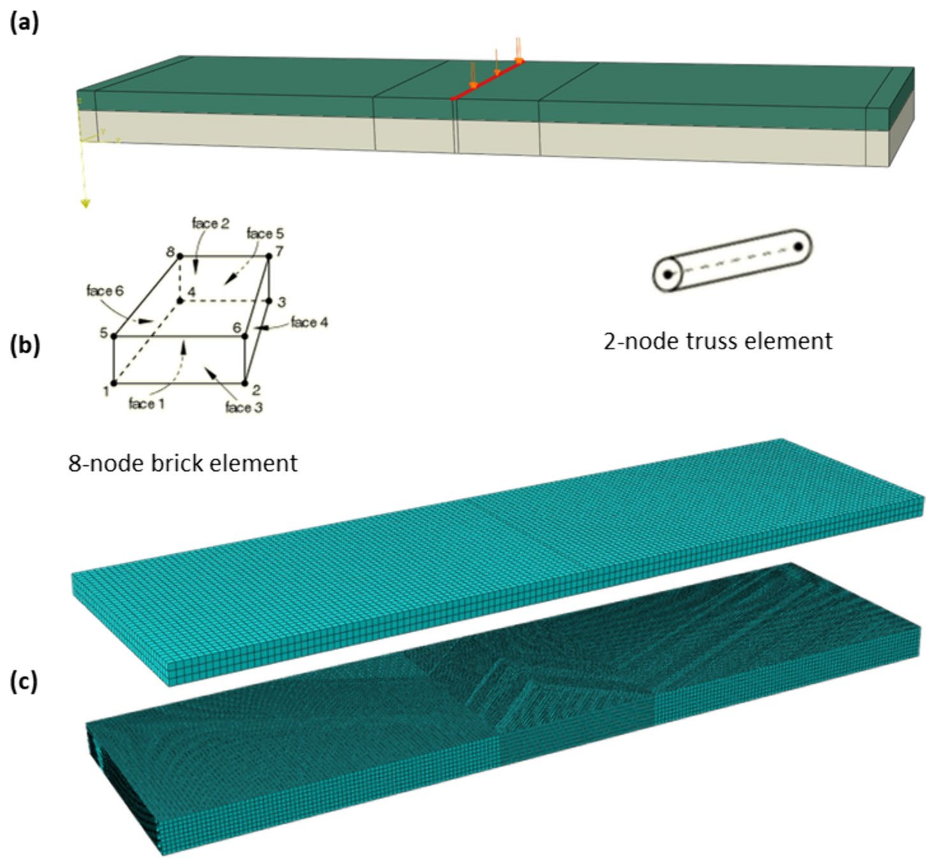

Fig. 4 Finite element model: **a** Parts. **b** Elements' type. **c** Meshing of slab and overlay

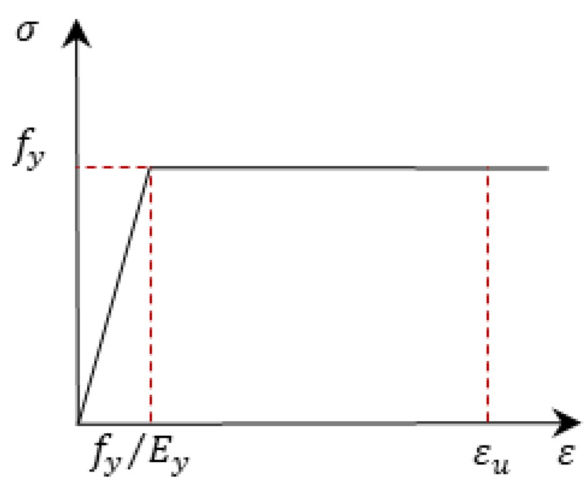

Fig. 5 Bi-linear model for reinforcing steel material

Modeling material properties

In his work, the steel reinforcement is modeled using a bi-linear model (Fig. 5). This model consists of two distinct branches. The initial branch is elastic, where the material can return to its original shape after the removal of load. This branch is characterized by a yield stress of 460 N/mm2 and a Poisson's ratio of 0.3. The subsequent branch is perfectly plastic, where any deformation in the material is irreversible.

In this study, the concrete damage plasticity (CDP) model in ABAQUS is used to simulate the nonlinear behavior of concrete. CDP model that was developed by Lubliner et al. [20] and modified later by Lee and Fenves [21]. The CDP model has been widely used in the simulation of concrete structures and has been shown to provide good agreement with experimental results [22, 23]. However, it should be noted that the accuracy of the model is highly dependent on the correct calibration of the material parameters (i.e., dilation angle, flow potential eccentricity, ratio of compressive strengths under biaxial to uniaxial loading, and viscosity). More details about CDP parameters are discussed elsewhere [17, 22].

The stress–strain behavior under sustained compressive loading is modeled in three phases (Fig. 6). The first two sections describe the ascending branch up to the peak stress. Their formulations are similar to the recommendations of the Model Code. The third and descending branch takes account of its dependency on the specimen geometry [24, 25] to ensure almost mesh-independent simulation results. The evolution of the compressive damage component d_c is linked to the corresponding compressive plastic strain and inelastic strain using a constant factor b_c of 0.7 [26].

The stress–strain relation for tensile loading consists of a linear branch up the tensile strength and a nonlinearly descending branch that derives from the stress-crack opening relation [27, 28] (Fig. 7). The damage parameter d_t depends on the tensile plastic strain and inelastic strain and a parameter b_t of 0.1 which assumes that strain to return back leaving only a small residual strain.

The modeling parameters for steel reinforcement and concrete are presented in Table 2.

Boundary conditions and loading

The slab is modeled as a simply supported slab with a distance of 190 cm between supports as shown in Fig. 3. A line load is applied at the center of the span, and the load is increased monotonically in small steps until failure, where the solution converges or the model terminates. The model is solved using the Full Newton–Raphson solver in ABAQUS [17].

Results and discussion

Original slab (OS)

The load–deflection curve in Fig. 8 compares the results of the finite element (FE) model with the experimental results. The comparison demonstrates a good correlation in the structural behavior of the system between the model and the experiments.

When considering the span/250 deflection limit [29] as a baseline to assess the gain in the structural capacity [10], it is observed that the corresponding load to this limit in the experiment is 8.8 kN, in comparison to 12 kN in the FE model. These values will serve as reference points for evaluating the effectiveness of this strengthening technique and the improvement in structural capacity.

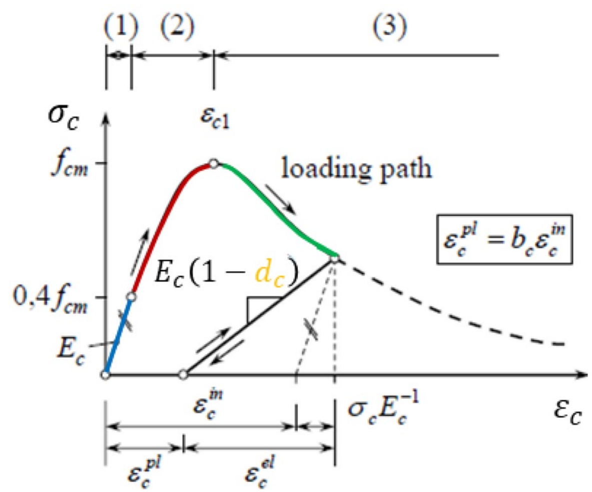

$$
\begin{cases}
\sigma_{c(1)} = E_c \varepsilon_c \\[2ex]
\sigma_{c(2)} = \dfrac{E_{ci} \frac{\varepsilon_c}{f_{cm}} - (\varepsilon_c / \varepsilon_{c1})^2}{1 + \left(E_{ci} \frac{\varepsilon_{c1}}{f_{cm}} - 2 \right) \frac{\varepsilon_c}{\varepsilon_{c1}}} f_{cm} \\[2ex]
\sigma_{c(3)} = \left(\dfrac{2 + \gamma_c f_{cm} \varepsilon_{c1}}{2 f_{cm}} - \gamma_c \varepsilon_c + \dfrac{\gamma_c {\varepsilon_c}^2}{2 \varepsilon_{c1}} \right)^{-1}
\end{cases}
$$

$$
d_c = 1 - \frac{\sigma_c E_c^{-1}}{\varepsilon_c^{pl} (1/b_c - 1) + \sigma_c E_c^{-1}}
$$

Fig. 6 Stress–strain relation for concrete in compression [26]

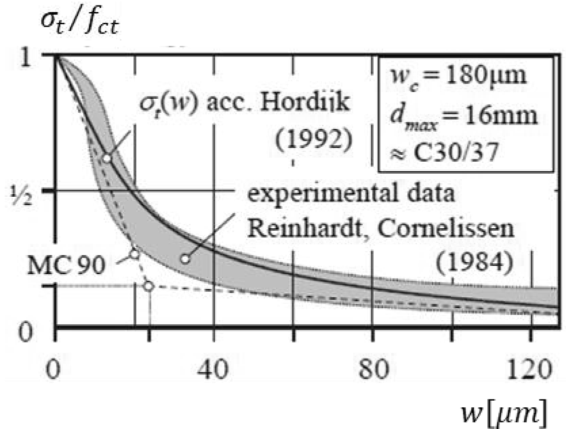

Fig. 7 Stress-crack opening and stress–strain relations concrete in tension [28]

$$\left\{\frac{\sigma_t(w)}{f_{ct}} = \left[1 + \left(\frac{3w}{w_c}\right)^3\right] e^{-6.93\frac{w}{w_c}} - 28\frac{w}{w_c} e^{-6.93}\right.$$

$$d_t = 1 - \frac{\sigma_t E_c^{-1}}{\varepsilon_t^{pl}(1/b_t - 1) + \sigma_t E_c^{-1}}$$

Table 2 Material properties in the model

Parameter	Value
Concrete	
Concrete Young's Modulus	24.1×10^3 N/mm^2
Concrete Poisson ratio	0.21
Dilation angle	40°
Flow potential eccentricity	0.12
Biaxial/uniaxial compression plastic strain ratio	1.16
Invariant stress ratio *Kc*	0.67
Viscosity	0.00001
Compression yield stress	30 N/mm^2
Inelastic strain	0
Tensile yield stress	3 N/mm^2
Tensile cracking strain	0
Steel reinforcement	
Steel Young's Modulus	2.1×10^5 N/mm^2
Steel Poisson ratio	0.3
Steel Yield stress	460 N/mm^2
Steel Plastic strain	0 `

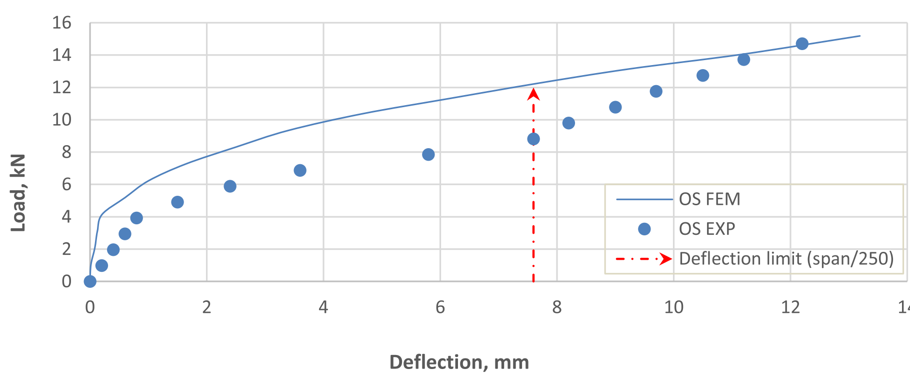

Fig. 8 Load mid-span deflection curve of the original slab in the model and experiments

The cracking pattern observed in both the FE model and the experiment (Fig. 9) is remarkably similar. The initial crack load recorded in the FE model is 9.35 KN, slightly higher than the experimental value of 8.8 KN.

Strengthened slab using concrete overlay and friction interface (SS-T6-Friction)

Figure 10 depicts the FE model of the strengthened slab using a concrete overlay with only a friction interface (SS-T6-Friction). The load–deflection correlation at mid-span shows good agreement with the experimental results, indicating an increased carrying capacity of the strengthened slab. The structural improvement in loads at the deflection limit and failure point of the strengthened slab in the FE model are 160% and 145% in comparison to 215% and 145% in the experiment, respectively, higher than those of the original slab.

In the FE model, the first crack load occurred at 13.8 KN, while in the experiment it occurred at 13.74 KN, demonstrating close agreement between the numerical and

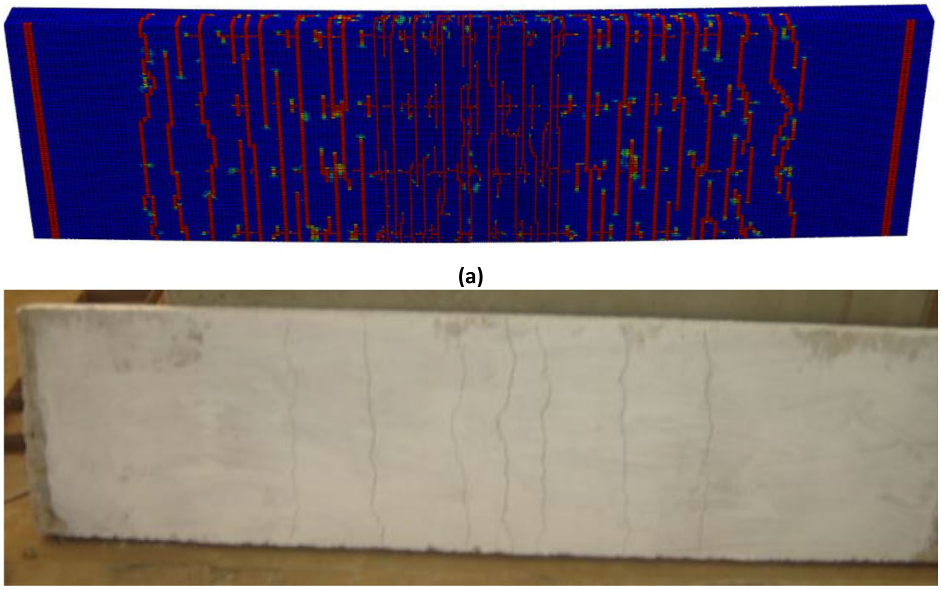

(a)

(b)

Fig. 9 Crack pattern of the original slab in **a** FE model and **b** experiment

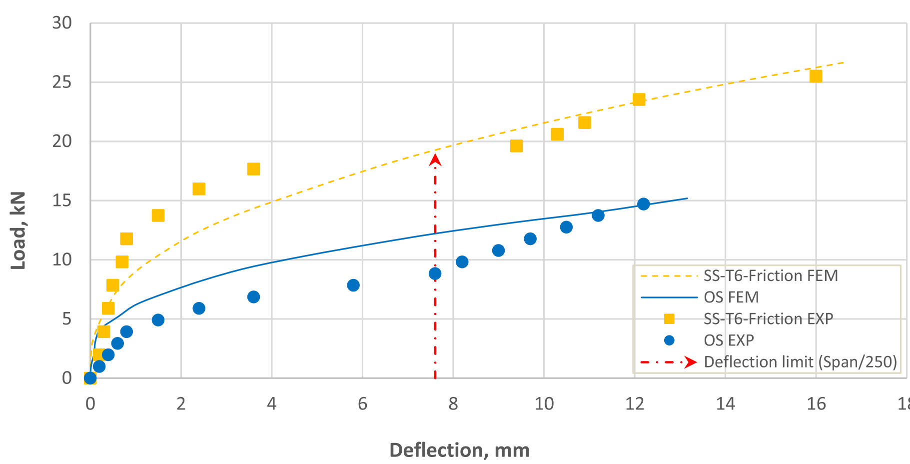

Fig. 10 Load mid-span deflection curve of the SS-T6-Friction slab vs original slab

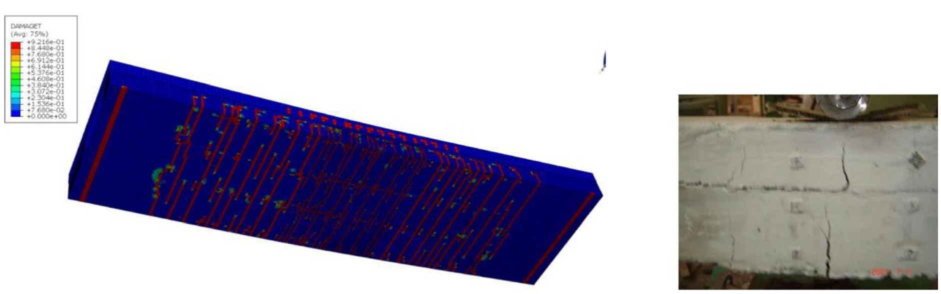

(a) **(b)**

Fig. 11 Cracking of the SS-T6-Friction slab in **a** FE model's crack pattern and **b** experiment crack at mid-span experimental values. Figure 11 compares the crack patterns observed in the FE models and at the mid-span.

As anticipated, without any bonding agent between the slab and concrete overlay, a slip occurred at the interface, as appeared in the FE displacement contour provided in Fig. 12, resulting in a displacement of 1.6 mm in the FE model. This behavior is also observed in the experimental results [2].

Strengthened slab using concrete overlay and epoxy adhesion at interface (SS-T6-Epoxy)

Figure 13 shows the FE model of the strengthened slab, SS-T6-Epoxy, which incorporates epoxy at the interface. The load–deflection correlation at the mid-point aligns favorably with the experimental results, with a maximum difference in load at the same mid-span deflection of approximately 9.8%.

In the FE model, the first crack load was observed at 12.85 KN, while in the experiments, it occurred at 19.6 KN. The crack pattern in the FE model of the strengthened slab is much closer to that observed in the experiment as shown in Fig. 14.

The carrying capacity of the strengthened slab, which utilizes an epoxy connection between the original slab and overlay, significantly increases when examining the relationship between load and mid-span deflection. The load at the span/250 deflection limit in the FE model rises to 32.4 kN (270%) compared to the experiment's 36 kN (400%), both surpassing the load of the original slab. This particular model of the strengthened slab exhibits minimal slip between the slab and overlay (Fig. 15), indicating full composite action, consistent with observations made during experiments [2].

Strengthened slab using concrete overlay and shear keys at interface (SS-T6-Shear Keys)

The load mid-span deflection relation in Fig. 16 of the FE model results for a one-way RC slab strengthened with an overlay using shear keys at the interface (SS-T6-Shear keys) demonstrates excellent agreement when compared to the previous experimental findings [2]. The maximum variance in load at mid-span deflection between the experimental and FE model curves was approximately 7.3%. In the FE model, the first crack load was observed at 18 kN, whereas in the experiment it occurred at 21.6 kN.

Figure 17 displays the crack patterns in the FE model as well as the crack at mid-span in the experiment. Similar to the experiment, slip was observed and predicted to be 1.7 mm in the developed model (Fig. 18).

At span/250 deflection limit, the load in the strengthened slab is estimated to be 28 kN in the FE model, while in the experiment it is measured as 26.58 kN. These results indicate an increase in structural capacity of 224% in both the FE model and the experimental work, demonstrating the effectiveness of this technique.

Strengthened slab using concrete overlay and shear keys at interface with additional reinforcement (SS-T8-Shear Keys)

In contrast to the previous slabs, the overlay in this slab is reinforced with T8@160 mm instead of T6@160 mm and shear keys. Figure 19 demonstrates a close match between the model and experimental results [2], with a maximum difference between the curves of approximately 20.4%. The FE model exhibited a first crack load

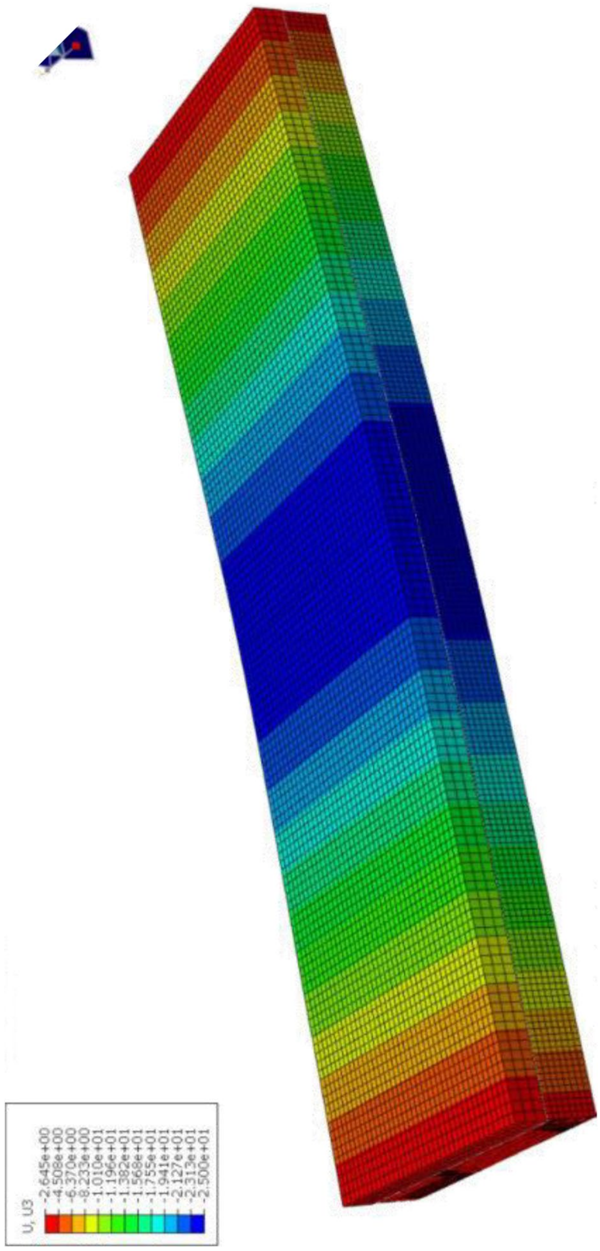

Fig. 12 Vertical displacement contour for SS-T6-Friction slab

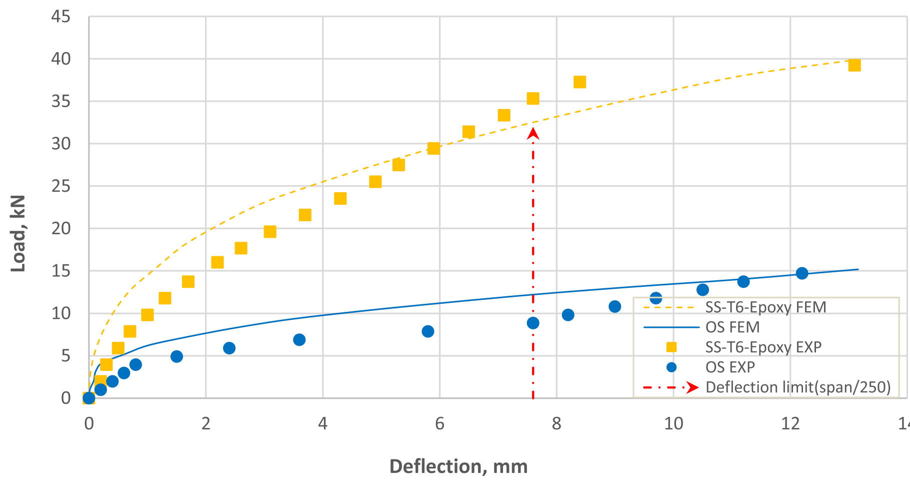

Fig. 13 Load mid-span deflection curve of the SS-T16-Epoxy slab vs original slab

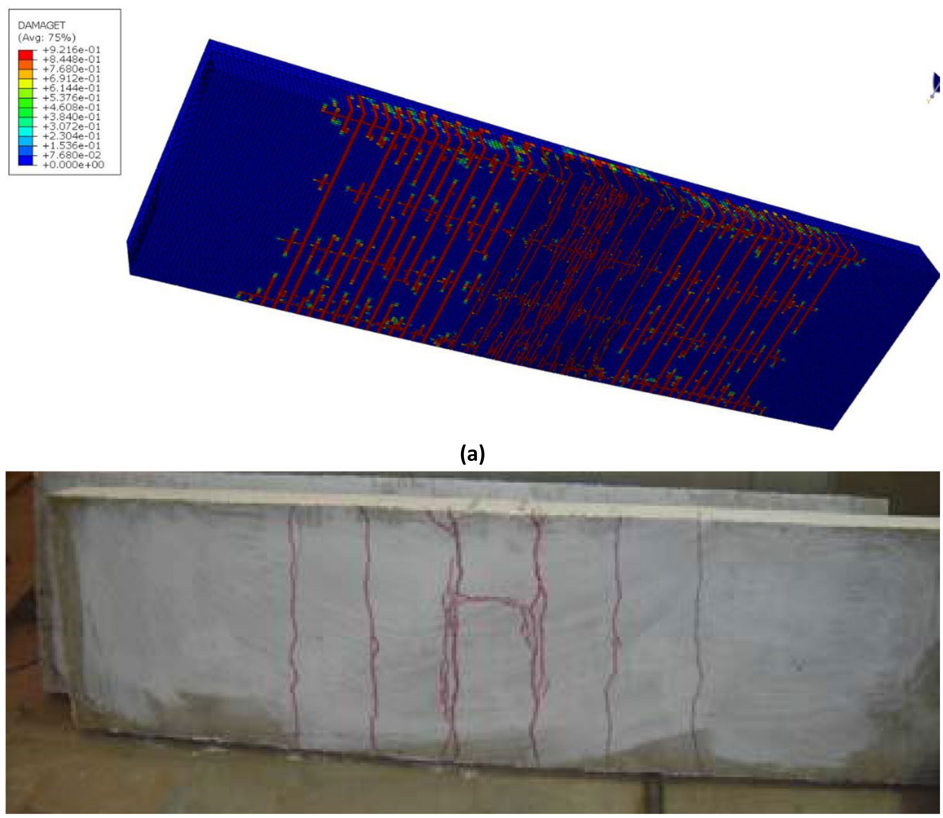

Fig. 14 Crack pattern of the SS-T16-Epoxy slab in **a** FE model and **b** experiment

of 19.73 KN, while the experimental test showed a first crack load of 13.74 KN, indicating similar cracks in both cases (Fig. 20).

The results demonstrate that the load at span/250 deflection limit, which was strengthened using an additionally reinforced overlay and shear keys (SS-T8-Shear

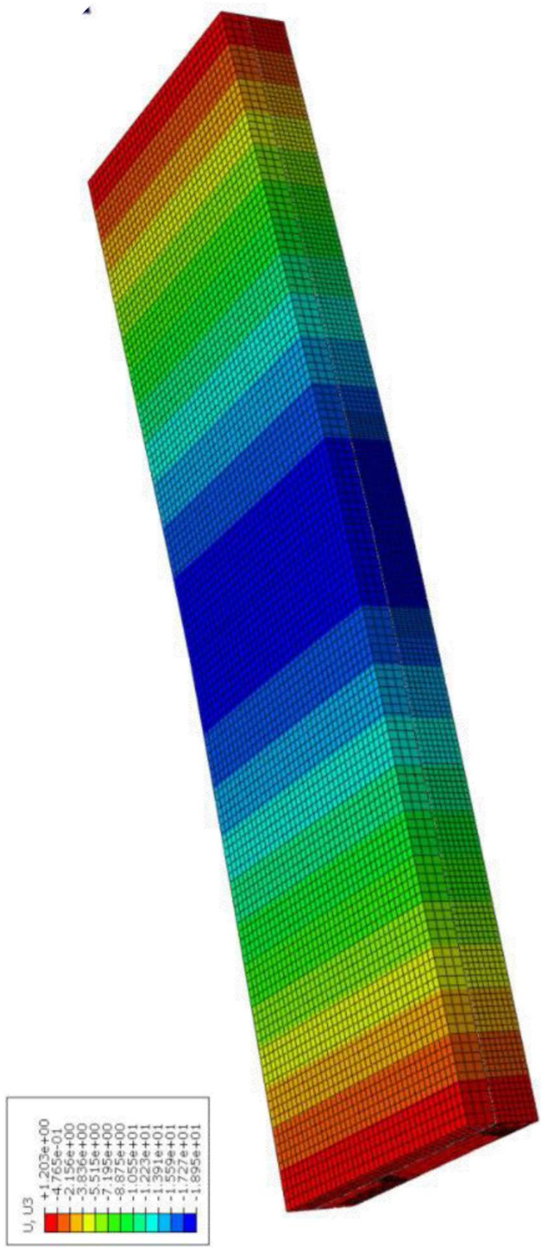

Fig. 15 Vertical displacement contour for SS-T6-Epoxy slab

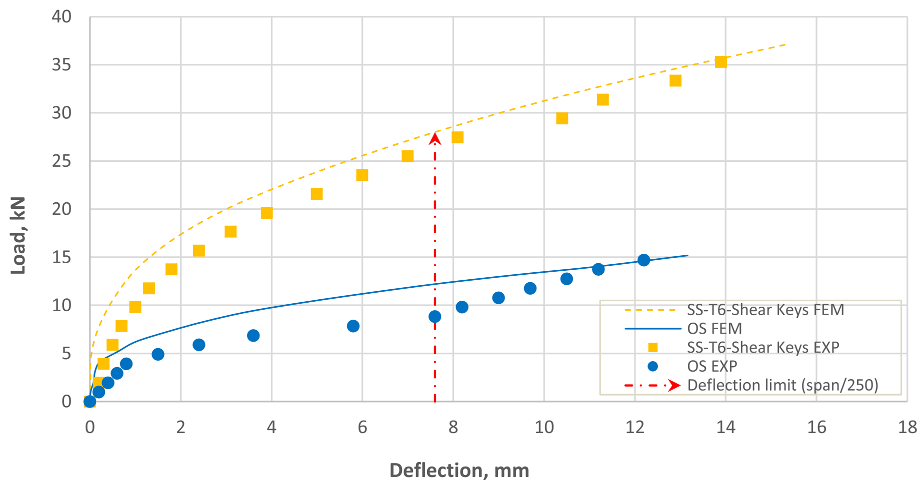

Fig. 16 Load vs mid-span deflection curve of the SS-T6-Shear keys slab vs original slab

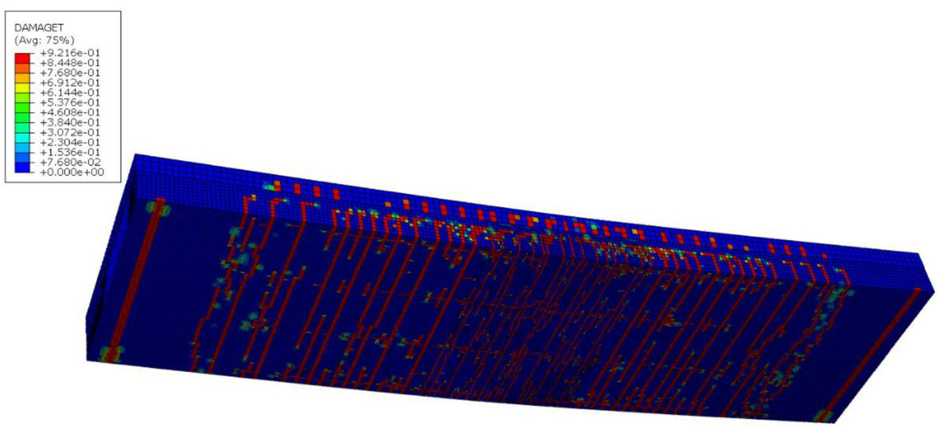

(a)

(b)

Fig. 17 Cracking of the SS-T6-Shear keys slab in **a** FE model's crack pattern and **b** experiment mid-span cracks

Keys), is 34.28 KN in the FE model, compared to 35.3 kN in the experiments. This represents a 400% and 285% increase, respectively, compared to the original slab. When comparing these results to those of SS-T6-Shear Keys slabs, it is evident that the additional reinforcement significantly enhances the structural capacity. However, these findings indicate that this technique improves the overall structural capacity.

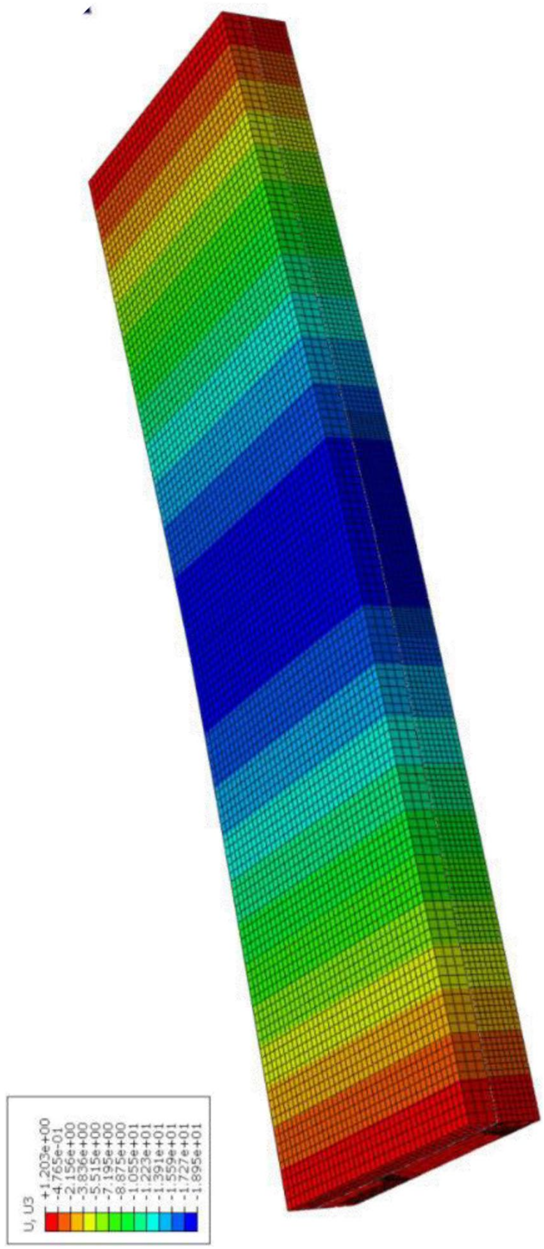

Fig. 18 Vertical displacement contour for SS-T6-Shear Keys slab

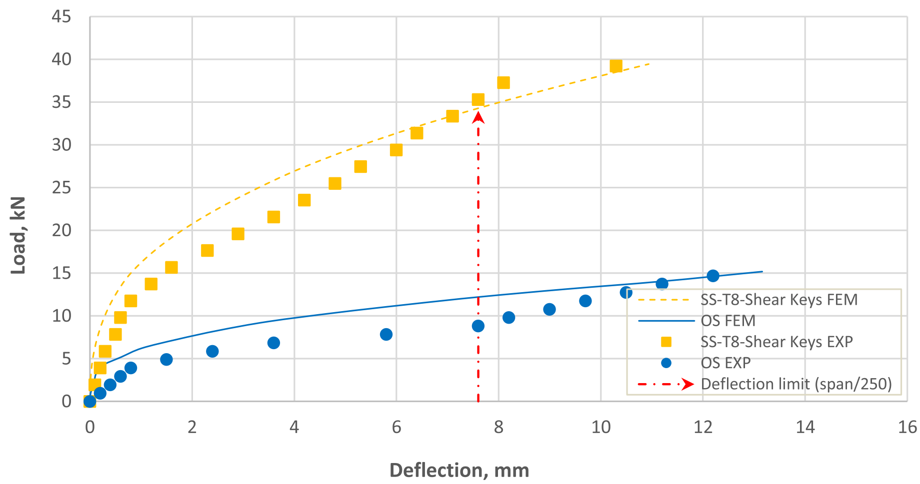

Fig. 19 Load vs mid-span deflection curve of the SS-T8-Shear keys slab vs original slab

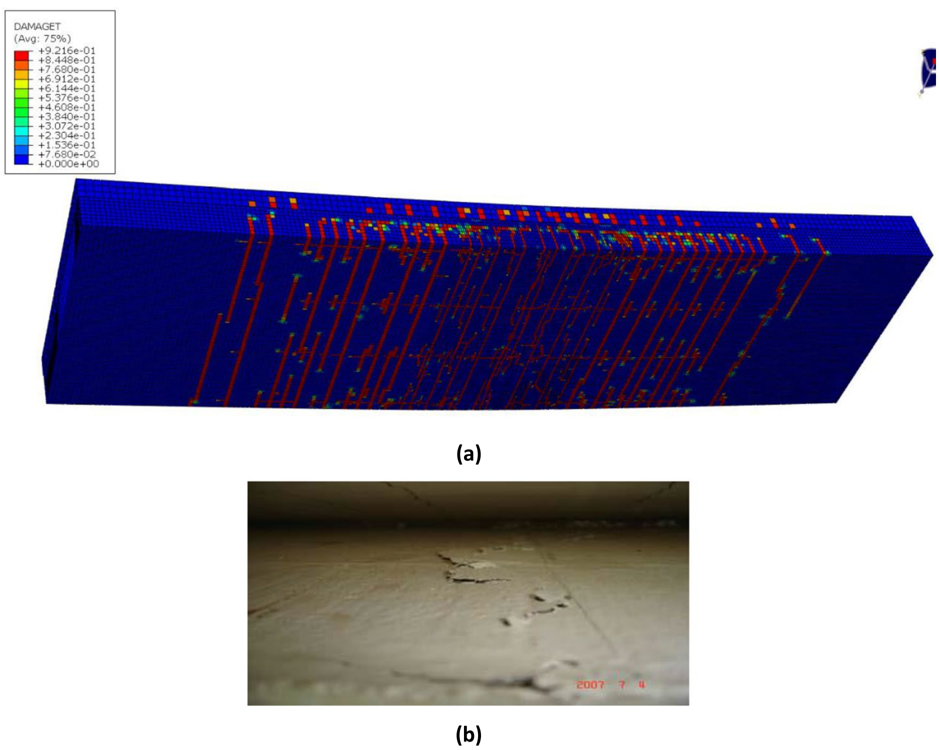

Fig. 20 Cracking of the SS-T8-Shear keys slab in **a** FE model's crack pattern and **b** experiment mid-span cracks

Both the experiment and FE model also show slip occurring between the slab and overlay at the supports, with a predicted slip of 1.28 mm in the FE model (Fig. 21).

Summary of the modeling results

Figure 22 compares the FE model results of the structural behavior of the strengthened slab using concrete overlay in comparison to the original slab. The comparison considers

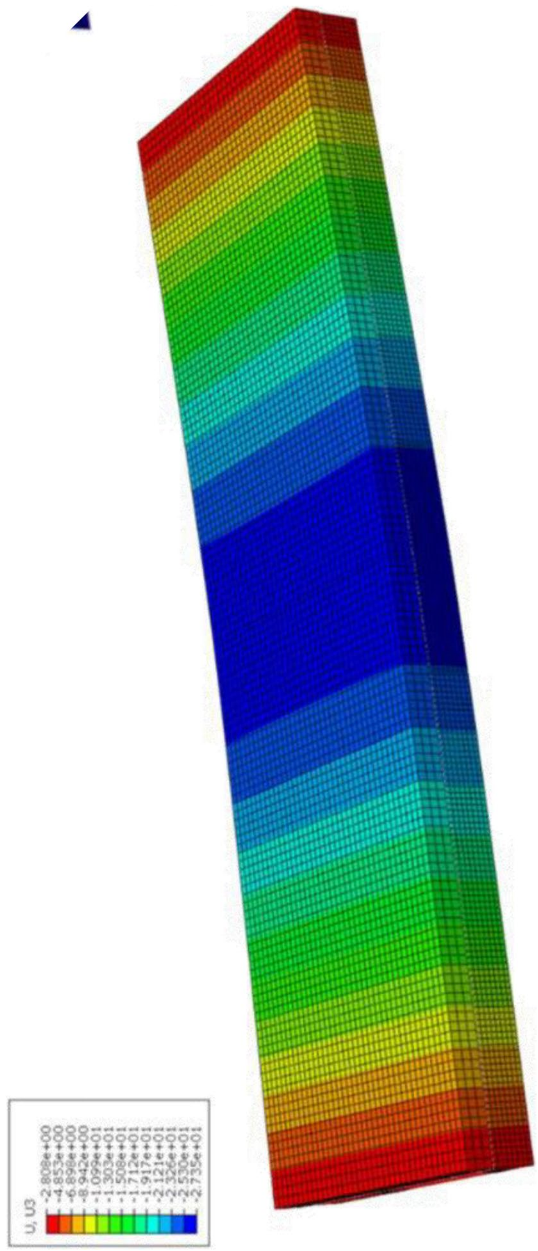

Fig. 21 Vertical displacement contour for SS-T8-Shear Keys slab

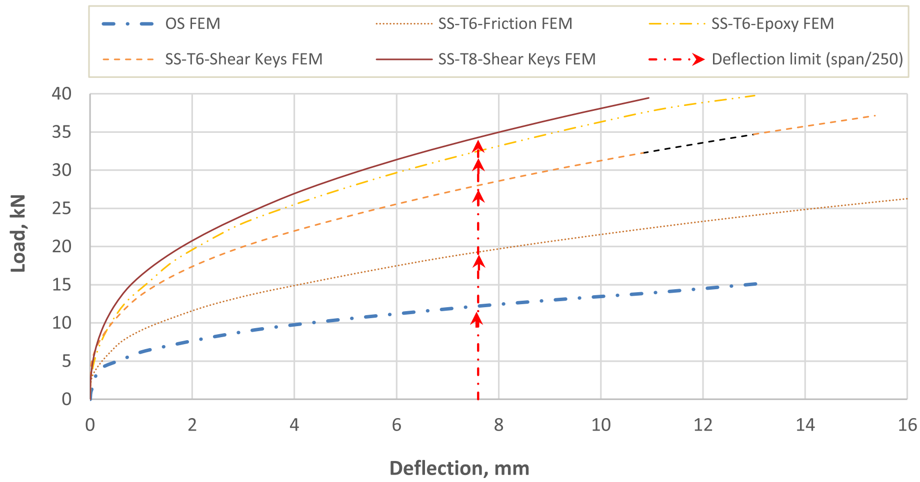

Fig. 22 Load–deflection curve of all slabs' FE models

Table 3 Comparison of the model's predicted and experimental loads at span/250 deflection limit

Slab	Load (kN)		Difference (%)
	Experiment	FE model	
SS-T6-Friction	19.0	19.2	1.2
SS-T6-Epoxy	35.3	32.5	-8.0
SS-T6-Shear keys	26.6	28.0	5.3
SS-T8-Shear keys	35.3	34.3	-2.9

four connections between the original slab and overlay: (1) no connection, relying solely on friction at the interface; (2) adhesive epoxy; (3) shear keys; and (4) shear keys with additional reinforcement in the overlay. A given deflection, for example, the deflection limit of span/250, the deflection is reached by a larger load in the strengthened slabs in comparison to the original slab. This is because the addition of the overlay necessarily increases the flexural stiffness and thereby decreases the deflection [30]. It is worth mentioning that the flexural stiffness is enhanced as high levels of composite action between the slab and overlay are achieved [16]. This is reflected in the results where the highest performance in the strengthened slabs is achieved in slabs that exhibited minimal slip, particularly, in the case of using adhesive epoxy and shear keys with additional reinforcement. In general, the results show a significant level of agreement between the FE model and experimental results, as presented in Table 3. All predicted load values from the FE model fall within 8% of the corresponding experimental values. These results demonstrate the accuracy of the developed model in replicating the load–deflection response, cracking behavior, and potential slip at the interface.

Conclusions

Based on the numerical results obtained in this study, the strengthened slabs using reinforced concrete overlay exhibited significant improvements in structural capacity. These findings are consistent with previous literature that has demonstrated the effectiveness of this technique. The developed 3D non-linear finite element model successfully simulated the structural behavior of the strengthened slabs. The model results closely matched the experimental data, indicating its accuracy and reliability. The predicted values from the model differed by less than 8% from the experimental values. Additionally, the model accurately captured the overall structural behavior, including the load–deflection curve, slip at the interface between the original slab and overlay, and crack pattern in the strengthened slabs. According to the results of this study, this modeling approach provided valuable insights into the process of slab strengthening with concrete overlays. The findings of this study contribute to our understanding of the effectiveness of this traditional strengthening technique and offer a useful tool for optimizing its design.

Acknowledgements
Not applicable.

Authors' contributions
Conceptualization, supervision, and final draft: A.O.A.; FE modeling study and preparation of the first draft: M.S. All authors have read and agreed to the published version of the manuscript.

Funding
No funding was obtained for this study.

Availability of data and materials
The data that support the findings are presented in the main body of this paper. The code that was used is available from the authors on a reasonable request.

Declarations

Competing interests
The authors declare that they have no competing interests.

Received: 9 December 2023 Accepted: 4 March 2024
Published online: 01 April 2024

References

1. ACI-546 (2014) ACI 546 guide to concrete repair
2. Abdelatif AO (2008) Flexural strengthening of one-way slabs using concrete overlay. MSc Thesis, University of Khartoum
3. Al-Kubaisy MA, Jumaat MZ (2000) Flexural behaviour of reinforced concrete slabs with ferrocement tension zone cover. Constr Build Mater 14:245–252
4. Oehlers D, Seracino R (2004) Design of FRP and steel plated RC structures: retrofitting beams and slabs for strength, stiffness and ductility. Elsevier
5. Krauser L (2006) Repairs, modifications, and strengthening with post-tensioning. PTI J 4:24–40
6. Mosallam AS, Mosalam KM (2003) Strengthening of two-way concrete slabs with FRP composite laminates. Constr Build Mater 17:43–54
7. Marzouk H, Ebead UA, Neale KW (2003) Flexural strengthening of two-way slabs using FRPs. In Fibre-Reinforced Polymer Reinforcement for Concrete Structures: (In 2 Volumes) (pp. 427–436)
8. Yu T, Teng JG, Wong YL, Dong SL (2010) Finite element modeling of confined concrete-I: Drucker-Prager type plasticity model. Eng Struct 32:665–79. https://doi.org/10.1016/j.engstruct.2009.11.014
9. Calixto JM, Pires EF, Lima SA, Piancastelli EM (2005) SP-229–25: Behavior of reinforced concrete slabs strengthened in flexure by concrete overlays. Qual Concr Struct Recent Adv Concr Mater Test; ACI Spec. Publ, vol 229. ACI, pp 389–406
10. Abdelatif AO, Wahab AA (2016) Flexural Strengthening of One-Way Slabs using Concrete Overlay. Sudan Eng Soc 62:17–21
11. Sirimontree S, Witchayangkoon B, Lertpocasombut K, Sornchomkaew P (2018) Strengthening of reinforced concrete slab by concrete overlay. MANZAR, Sci J Landsc 10:60–7. https://doi.org/10.22034/manzar.2018.76866
12. Ibrahim W, El-Adawy M, Ghanem G (2014) Behaviour of reinforced concrete slabs strengthened by concrete overlays. Constr Mater Struct :956–62. https://doi.org/10.3233/978-1-61499-466-4-956
13. Perez F, Bissonnette B, Gagné R (2009) Parameters affecting the debonding risk of bonded overlays used on reinforced concrete slab subjected to flexural loading. Mater Struct 42:645–662
14. El-Mandouh MA, Elsamak G, Rageh BO, Hamoda A, Abdelazeem F (2023) Experimental and numerical investigation of one-way reinforced concrete slabs using various strengthening systems. Case Stud Constr Mater 18:e01691
15. Helsel MA, Muñoz JF, Haber ZB, De la Varga I (2023) Effect of bridge deck surface preparation on the consolidation and bond of UHPC overlays. Constr Build Mater 364:129860

16. Abdelatif AO, Mustafa M, Kabosh MA (2021) Modelling of structural behaviour in strengthened reinforced concrete one-way slabs using concrete overlay. Univ Khartoum Eng J 11:27–33
17. Abaqus CDSS, CAE, (2017) User's Guide. Abaqus/CAE Stand 2017:2017
18. Sinaei H, Shariati M, Abna AH, Aghaei M, Shariati A (2012) Evaluation of reinforced concrete beam behaviour using finite element analysis by ABAQUS. Sci Res Essays 7:2002–2009
19. Pedro M, Eduardo N (2010) Assessment of the shear strength between concrete layers. Proc. 8th fib PhD Symp. Kgs, Lyngby, Denmark. pp 20–3
20. Lubliner J, Oliver J, Oller S, Onate E (1989) A plastic-damage model for concrete. Int J Solids Struct 25:299–326
21. Lee J, Fenves GL (1998) Plastic-damage model for cyclic loading of concrete structures. J Eng Mech 124:892
22. Abdelatif AO, Owen JS, Hussein MFM (2015) Modelling the prestress transfer in pre-tensioned concrete elements. Finite Elem Anal Des 94:47–63. https://doi.org/10.1016/j.finel.2014.09.007
23. Abdelatif AO, Owen JS, Hussein MFM (2017) Modelling and parametric study of the re-anchorage of ruptured tendons in bonded post-tensioned concrete. J Struct Eng 143:04017162
24. Van Mier JGM (1984) Strain-softening of concrete under multiaxial loading conditions. Doctoral dissertation, Technical University of Eindhoven
25. Vonk RA (1993) A micromechanical investigation of softening of concrete loaded in compression. Heron 38:3–94
26. Sinha BP, Gerstle KH, Tulin LG (1964) Stress-strain relations for concrete under cyclic loading. Am Concr Inst J 61(2):195–212
27. Hordijk DA (1992) Tensile and tensile fatigue behaviour of concrete; experiments, modeling and analyses. Heron 37:3–79
28. Reinhardt HW, Cornelissen HAW (1984) Post-peak cyclic behaviour of concrete in uniaxial tensile and alternating tensile and compressive loading. Cem Concr Res 2:263–270
29. BSI (1997) BS8110, Structural use of concrete, part 1: Code of practice for design and construction. British Standards Institution, UK
30. Ibrahim N, Kabosh MA, Abdelatif AO (2020) Modeling Deflection in Reinforced Concrete One-way Slabs using Eurocode2 Model. FES J Eng Sci 9:91–95

Publisher's Note